Article

Determination of the Absolute Configuration of [3](1,4)Barrelenophanedicarbonitrile Using Concerted Time-Dependent Density Functional Theory Calculations of Optical Rotation and Electronic Circular Dichroism

P. J. Stephens, D. M. McCann, F. J. Devlin, J. R. Cheeseman, and M. J. Frisch

J. Am. Chem. Soc., **2004**, 126 (24), 7514-7521• DOI: 10.1021/ja049185q • Publication Date (Web): 28 May 2004

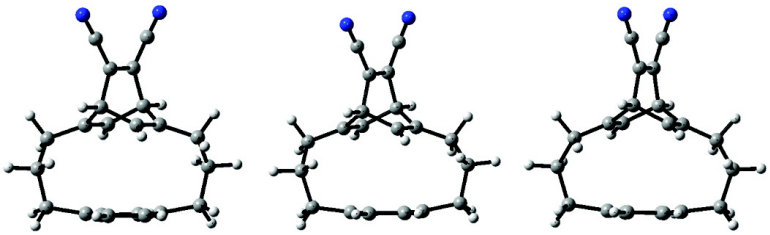

(R,R)-(-)-[3_2](1,4)Barrelenophanedicarbonitrile

More About This Article

Additional resources and features associated with this article are available within the HTML version:

- Supporting Information
- Links to the 12 articles that cite this article, as of the time of this article download
- Access to high resolution figures
- Links to articles and content related to this article
- Copyright permission to reproduce figures and/or text from this article

View the Full Text HTML

J|A|C|S
ARTICLES
Published on Web 05/28/2004

Determination of the Absolute Configuration of [3_2](1,4)Barrelenophanedicarbonitrile Using Concerted Time-Dependent Density Functional Theory Calculations of Optical Rotation and Electronic Circular Dichroism

P. J. Stephens,*,† D. M. McCann,† F. J. Devlin,† J. R. Cheeseman,‡ and M. J. Frisch‡

Contribution from the Department of Chemistry, University of Southern California, Los Angeles, California 90089-0482, and Gaussian Inc., 340 Quinnipiac Street, Building 40, Wallingford, Connecticut 06492-4050

Received February 13, 2004; E-mail: pstephen@usc.edu

Abstract: The technique of time-dependent density functional theory (TDDFT) has very recently been applied to the calculation of both transparent spectral region optical rotations and electronic circular dichroism (CD). Here, we report the *concerted* application of the new methodologies to the determination of the absolute configuration (AC) of [3_2](1,4)barrelenophanedicarbonitrile, **1**, the first optically active barrelenophane. **1** is conformationally flexible: the two three-carbon bridges of **1** can each exhibit two conformations, leading to three inequivalent conformations of **1**: **a**, **b**, and **c**. Conformational structures and energies are predicted using DFT at the B3LYP/6-31G* level. Comparison of the calculated structures to structures obtained via X-ray crystallography of (+)-**1** shows that (remarkably) *all three conformations* **a**−**c** are simultaneously present in crystalline (+)-**1**. The sodium D line specific rotations, $[\alpha]_D$, and CD spectra of **a**−**c** are calculated using TDDFT at the B3LYP/aug-cc-pVDZ level. Comparison of the conformationally averaged specific rotation and CD spectrum to the experimental data of Matsuda-Sentou and Shinmyozu leads to the AC 9S,12S(+)/9R,12R(−). The same AC is obtained both from $[\alpha]_D$ and from the CD, strongly supporting its reliability.

Introduction

Chiral molecules exhibit optical activity: optical rotation and circular dichroism. Enantiomers of a chiral molecule exhibit optical rotation and circular dichroism (CD) of equal magnitude and opposite sign at any frequency. Mirror-image enantiomers thus exhibit mirror-image optical rotatory dispersion and circular dichroism spectra. It follows that the absolute configuration of a chiral molecule can in principle be obtained from measurements of optical rotation and/or circular dichroism. In practice, this requires a theoretical methodology reliably relating optical activity and molecular structure. Very recently, dramatic advances have occurred in the theoretical prediction of the optical rotation and circular dichroism originating in electronic excitations. The technique of time-dependent density functional theory (TDDFT) has been applied to the calculation of both electronic optical rotation and electronic circular dichroism.[1] In the former case, optical rotations are calculated in transparent spectral regions (i.e., outside of regions of absorption). In the latter case, energies and rotational strengths of electronic excitations are calculated. The reliability of the new TDDFT methods, to the extent documented to date, is very encouraging.[1,2] As a result, it is now possible to determine absolute configurations (ACs) with considerable confidence using TDDFT calculations of optical rotation and/or circular dichroism.

To date, applications of this new methodology are quite sparse in number[3] and have used either optical rotation or circular dichroism, but not both. When both optical rotation and circular dichroism are measurable, however, the reliability of the AC determined is greatly enhanced by the simultaneous use of both phenomena. When theoretical predictions, using the same

† University of Southern California.
‡ Gaussian Inc.

(1) (a) Stephens, P. J.; Devlin, F. J.; Cheeseman, J. R.; Frisch, M. J. *J. Phys. Chem. A* **2001**, *105*, 5356. (b) Mennucci, B.; Tomasi, J.; Cammi, R.; Cheeseman, J. R.; Frisch, M. J.; Devlin, F. J.; Gabriel, S.; Stephens, P. J. *J. Phys. Chem. A* **2002**, *106*, 6102. (c) Grimme, S. *Chem. Phys. Lett.* **2001**, *339*, 380. (d) Grimme, S.; Furche, F.; Ahlrichs R. *Chem. Phys. Lett.* **2002**, *361*, 321. (e) Autschbach, J.; Patchkovskii, S.; Ziegler, T.; van Gisbergen, S. J. A.; Baerends, E. J. *J. Chem. Phys.* **2002**, *117*, 581. (f) Ruud, K.; Helgaker, T. *Chem. Phys. Lett.* **2002**, *352*, 533. (g) Furche, F.; Ahlrichs, R.; Wachsmann, C.; Weber, E.; Sobanski, A.; Vogtle, F.; Grimme, S. *J. Am. Chem. Soc.* **2000**, *122*, 1717. (h) Autschbach, J.; Ziegler, T.; van Gisbergen, S. J. A.; Baerends, E. J. *J. Chem. Phys.* **2002**, *116*, 6930.
(2) (a) Stephens, P. J.; Devlin, F. J.; Cheeseman, J. R.; Frisch, M. J.; Mennucci, B.; Tomasi, J. *Tetrahedron Asymmetry* **2000**, *11*, 2443. (b) Stephens, P. J.; Devlin, F. J.; Cheeseman, J. R.; Frisch, M. J. *Chirality* **2002**, *14*, 288. (c) Grimme, S.; Bahlmann, A.; Haufe, G. *Chirality* **2002**, *14*, 793. (d) Polavarapu, P. L. *Chirality* **2002**, *14*, 768. (e) Polavarapu, P. L.; Petrovic, A.; Wang, F. *Chirality* **2003**, *15*, S143. (f) Wiberg, K. H.; Vaccaro, P. H.; Cheeseman, J. R. *J. Am. Chem. Soc.* **2003**, *125*, 1888. (g) Diedrich, C.; Grimme, S. *J. Phys. Chem. A* **2003**, *107*, 2524.
(3) (a) Stephens, P. J.; Devlin, F. J.; Cheeseman, J. R.; Frisch, M. J.; Rosini, C. *Org. Lett.* **2002**, *4*, 4595. (b) Stephens, P. J.; Devlin, F. J.; Cheeseman, J. R.; Frisch, M. J.; Bortolini, O.; Besse, P. *Chirality* **2003**, *15*, S57. (c) Wang, F.; Wang, Y.; Polavarapu, P. L.; Li, T.; Drabowicz, J.; Pietrusiewicz, K. M.; Zygo, K. *J. Org. Chem.* **2002**, *67*, 6539. (d) Polavarapu, P. L. *Angew. Chem., Int. Ed.* **2002**, *41*, 4544. (e) Wang, Y.; Raabe, G.; Repges, C.; Fleischhauer, J. *Int. J. Quantum Chem.* **2003**, *93*, 265.

 10.1021/ja049185q CCC: $27.50

methodology, are in agreement with experiment for both phenomena, the AC is substantially more definitive than when only one phenomenon is used. Conversely, if the use of optical rotation and circular dichroism yield opposite ACs, the AC determined using either phenomenon is unreliable.

Here, we report the first application of *concerted* TDDFT calculations of optical rotation and circular dichroism to the determination of the AC of a chiral molecule whose AC has to date not been assigned.[4] The molecule studied is a chiral barrelenophane: [3_2](1,4)barrelenophanedicarbonitrile, **1**:

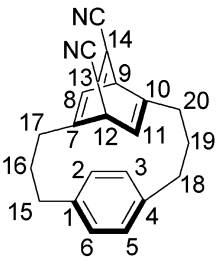

9R,12R-**1**

The resolution of the enantiomers of **1** via chiral chromatography was recently reported by Matsuda-Sentou and Shinmyozu.[5] Specific rotations, $[\alpha]_D$, and near-UV (250−450 nm) circular dichroism spectra for the two enantiomers were reported. The X-ray structure of (+)-**1** was also reported. However, the AC of **1** was not obtained. X-ray crystallography did not provide the AC as a result of the absence of "heavy" atoms in **1** and of the presence of disorder in the structure. No attempt was made to extract the AC from the optical rotation or circular dichroism data. In this work, we have predicted the specific rotation $[\alpha]_D$ and the near-UV circular dichroism spectrum of **1** using TDDFT. Comparison to the experimental data of Matsuda-Sentou and Shinmyozu yields the AC. Identical ACs are provided by the two phenomena, which in turn strongly supports the reliability of the AC arrived at.

The barrelenophane, **1**, is a flexible molecule: multiple conformations are possible. Conformational analysis is prerequisite to the calculation of optical rotation and circular dichroism and, thence, AC determination. In this work, conformational analysis is carried out using density functional theory (DFT). The reliability of the conformational structures obtained is assessed by comparison to structures obtained using X-ray crystallography.

Methods

Conformational analysis of **1** has been carried out in two ways. First, Monte Carlo conformational searching using both the MMFF94 molecular mechanics force field[6] and the AM1 semiempirical method[7] has been carried out using Spartan 02.[8] The structures of the stable conformations obtained were further optimized using ab initio DFT, together with the functional B3LYP and the basis set 6-31G*, via Gaussian 98 or 03.[9] Second, systematic conformational searching has been carried out using DFT (B3LYP/6-31G*) and Gaussian 98 or 03. For all conformations, B3LYP/6-31G* frequency calculations were carried out using Gaussian 98 or 03, confirming that the conformations are stable, and free energies were calculated.

Specific rotations at the sodium D line, $[\alpha]_D$, have been calculated for each stable conformation using TDDFT and Gaussian 03.[9] The methodology uses gauge-invariant (including) atomic orbitals (GIAOs), ensuring origin-independent rotations.[10] The functional and basis set were B3LYP and aug-cc-pVDZ, respectively, a combination of choices whose accuracy in predicting optical rotations has been thoroughly documented.[1a] Specific rotations were calculated at B3LYP/6-31G* equilibrium geometries.

Electronic excitation energies and rotational strengths have been calculated using TDDFT and Gaussian 03.[9] GIAOs are not used in calculating rotational strengths. Electric dipole transition moments are calculated using both "length" and "velocity" representations. Length and velocity rotational strengths are origin-dependent and -independent, respectively, except at the complete basis set limit when they are equal and origin-independent. The origin used was the center of positive charge. The functional and basis set were B3LYP and aug-cc-pVDZ, respectively, for consistency with the optical rotation calculations. Equilibrium geometries were again B3LYP/6-31G*.

Table 1. Conformational Energies and Populations of **1**[a]

	ΔE			ΔG	x^b	x^c
	MMFF94	AM1	B3LYP/6-31G*	B3LYP/6-31G*	(ΔE)	(ΔG)
a	0.00	0.48	0.00	0.00	54.5	64.8
b	0.11	0.48	0.25	0.46	35.9	29.7
c	0.41	0.00	1.03	1.46	9.6	5.5

[a] Relative energies in kilocalories per mole. Populations in percent. [b] Based on B3LYP/6-31G* ΔE values. $T = 298$ K. [c] Based on B3LYP/6-31G* ΔG values. $T = 298$ K.

Results

Conformational Analysis. Conformational analysis of **1** was initially carried out using Monte Carlo conformational searching, together with the MMFF94 molecular mechanics and AM1 semiempirical methods. MMFF94 and AM1 structures were reoptimized using ab initio DFT at the B3LYP/6-31G* level. Three stable conformations, **a**, **b**, and **c**, were identified; their relative energies are listed in Table 1. MMFF94 and B3LYP/6-31G* calculations result in the energy ordering: **a** < **b** < **c**. AM1 gives a different order: **c** < **a** ≈ **b**. For the B3LYP/6-31G* structures, relative free energies have also been calculated, with the results given in Table 1.

The B3LYP/6-31G* structures of conformations **a**−**c** of 9R,12R-**1** (henceforth, R,R-**1**) are shown in Figure 1. Conformations **a** and **c** exhibit C_2 symmetry; **b** has C_1 symmetry. The differences in geometry between conformations **a**, **b**, and **c** lie predominantly in the conformations of the two three-carbon bridges. These bridges each exhibit two conformations. In **a**

(4) For concerted TDDFT calculations of the optical rotations and circular dichroism spectra of four bicyclo[3.3.1]nonanediones whose ACs had been assigned previously, see: Stephens, P. J.; McCann, D. M.; Butkus, E.; Stončius, S.; Cheeseman, J. R.; Frisch, M. J. *J. Org. Chem.* **2004**, *69*, 1948.
(5) Matsuda-Sentou, W.; Shinmyozu, T. *Tetrahedron: Asymmetry* **2001**, *12*, 839.
(6) MMFF94: Halgren, T. A. *J. Comput. Chem.* **1996**, *17*, 490.
(7) AM1: Dewar, M. J. S.; Zoebisch, E. G.; Healey, E. F.; Stewart, J. J. P. *J. Am. Chem. Soc.* **1985**, *107*, 3902.
(8) *Spartan 02*; Wavefunction Inc., Irvine, CA.
(9) Frisch, M. J.; Trucks, G. W.; Schlegel, H. B.; Scuseria, G. E.; Robb, M. A.; Cheeseman, J. R.; Zakrzewski, V. G.; Montgomery, J. A., Jr.; Stratmann, R. E.; Burant, J. C.; Dapprich, S.; Millam, J. M.; Daniels, A. D.; Kudin, K. N.; Strain, M. C.; Farkas, O.; Tomasi, J.; Barone, V.; Cossi, M.; Cammi, R.; Mennucci, B.; Pomelli, C.; Adamo, C.; Clifford, S.; Ochterski, J.; Petersson, G. A.; Ayala, P. Y.; Cui, Q.; Morokuma, K.; Malick, D. K.; Rabuck, A. D.; Raghavachari, K.; Foresman, J. B.; Cioslowski, J.; Ortiz, J. V.; Stefanov, B. B.; Liu, G.; Liashenko, A.; Piskorz, P.; Komaromi, I.; Gomperts, R.; Martin, R. L.; Fox, D. J.; Keith, T.; Al-Laham, M. A.; Peng, C. Y.; Nanayakkara, A.; Gonzalez, C.; Challacombe, M.; Gill, P. M. W.; Johnson, B. G.; Chen, W.; Wong, M. W.; Andres, J. L.; Head-Gordon, M.; Replogle, E. S.; Pople, J. A. *Gaussian 98* and *03*; Gaussian, Inc.: Pittsburgh, PA.
(10) Cheeseman, J. R.; Frisch, M. J.; Devlin, F. J.; Stephens, P. J. *J. Phys. Chem. A* **2000**, *104*, 1039.

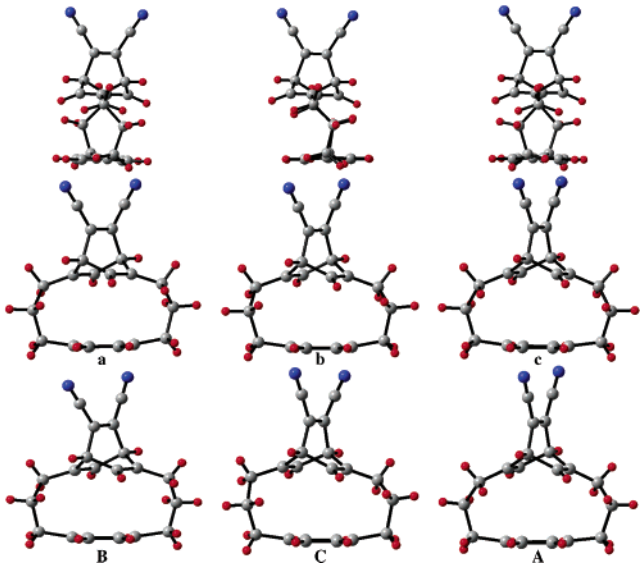

Figure 1. B3LYP/6-31G* structures of conformations **a**, **b**, and **c** of R,R-**1** and X-ray structures **B**, **C**, and **A** of (+)-**1**. Conformations **a**, **b**, and **c** are viewed from two directions in order to demonstrate the conformations of the two three-carbon bridges.

Table 2. Calculated Dihedral Angles of **1**[a]

	a	b	c
C10−C20−C19−C18	−82.6	87.2	88.4
C20−C19−C18−C4	63.4	−58.2	−56.1
C7−C17−C16−C15	−82.6	−76.7	88.4
C17−C16−C15−C1	63.4	70.3	−56.1

[a] In degrees, for B3LYP/6-31G* geometries of R,R-**1**. For atom numbering, see text.

and **c**, the conformations of the two bridges are the same i.e., superposable under C_2 rotation. In **b** the conformations are different. A more detailed characterization of the structures of **a**−**c** is provided by the dihedral angles of the C atoms of the two bridges, listed in Table 2.

In order to confirm the Monte Carlo-based conformational analysis and to further define the barriers to interconversion among the three conformations, we have scanned the B3LYP/6-31G* potential energy surface (PES) of **1**, varying simultaneously the two dihedral angles C7C17C16C15 and C10C20C19C18. The PES is given in Figure 2. There are four valleys in the PES. The C_2 symmetry line corresponding to C7C17C16C15 = C10C20C19C18 passes through two valleys. Structures **a** and **c** lie within these valleys. The other two valleys are not on the C_2 symmetry line. Structure **b** lies within these valleys; the two valleys correspond to the two orientations of **b**, interconverted by a 180° rotation. The conformation in which C7C17C16C15 = C10C20C19C18 = 0 corresponds to a maximum in the PES, >20 kcal higher than structure **a**. Structures **a**, **b**, and **c** are separated by saddle points whose energies are 10−14 kcal higher than structure **a**.

X-ray Crystal Structures of 1. Crystals of racemic-**1** and of (+)-**1** have been characterized via X-ray crystallography.[5,11] In both structures there are four molecules per unit cell. In (+)-**1**, the four molecules are inequivalent;[5] in racemic **1** they are equivalent.[11] In (+)-**1**, one of the three-carbon bridges of one of the four molecules is disordered; in racemic **1**, one of the three-carbon bridges is disordered in all four molecules. Comparison of the structures defined via X-ray crystallography for (+)-**1** to the B3LYP/6-31G* structures of conformations **a**−**c** leads to the conclusion that the three molecules labeled **A**, **B**, and **C** exhibit the conformations **c**, **a**, and **b**, respectively. Experimental and calculated structures are compared qualitatively in Figure 1. Quantitative comparison of the dihedral angles of the three-carbon bridges is made in Table 3 and Figure 3. The average absolute deviation of calculated dihedral angles from experimental angles for the three molecules **A**, **B**, and **C** is 3.3°. In the case of molecule **D**, all three C atoms of one bridge, labeled C83, C84, and C85 by Matsuda-Sentou and Shinmyozu,[5] are reported to be disordered. The disorder is consistent with a superposition of conformations **a** and **b**, atoms C83A, C84A, and C85A being assigned to C17, C16, and C15 of **a** and C83B, C84B, and C85B being assigned to C17, C16, and C15 of **b**. This assumption yields the dihedral angles given in Table 3 and Figure 3. The agreement between theory and experiment is comparable to that for molecules A, B, and C. The average absolute deviation of dihedral angles for molecules **A**, **B**, **C**, and **D** together is 4.1°. In the case of racemic-**1**, all four molecules in the unit cell are disordered. The agreement between calculated and experimental dihedral angles, assuming a mixture of conformations **b** and **c**, is less good than that for the (+)-**1** structures (Table 3). Reexamination of the X-ray analysis of (±)-**1** in the light of our calculational results would be of interest.

Assigning conformations **c**, **a**, and **b** to molecules **A**, **B**, and **C** of (+)-**1**, we have also compared calculated and experimental bond lengths and bond angles (Tables 1 and 2 and Figures 1 and 2 of Supporting Information). Agreement is good: average absolute deviations of bond lengths/bond angles for molecules **A**, **B**, and **C** are 0.015 Å/0.8°, 0.012 Å/0.8°, and 0.014 Å/0.8°, respectively. In addition, we have compared calculated and experimental distances between C atoms of the barrelene and phenyl rings, with the results given in Table 4. Calculated interatomic distances are uniformly larger than experimental distances; the average deviation is 0.09 Å.

Optical Rotation. We have predicted the sodium D line-specific rotation of **1** using the ab initio TDDFT/GIAO methodology implemented in Gaussian 03. $[\alpha]_D$ values calculated using the B3LYP functional and the aug-cc-pVDZ basis set for each of the three conformations, **a**−**c**, are given in Table 5. For each conformation, the B3LYP/6-31G* geometry is used. For R,R-**1**, $[\alpha]_D$ values are negative for **a** and **b** and positive for **c**. The $[\alpha]_D$ value of the equilibrium mixture of conformations is

$$[\alpha]_D = \sum_i x_i [\alpha]_D^i$$

where x_i is the fractional population of conformation i whose $[\alpha]_D$ value is $[\alpha]_D^i$. Populations, x_i, are calculated from the B3LYP/6-31G* relative free energies, ΔG_i, using Boltzmann statistics, with the results listed in Table 1. These in turn lead to a conformationally averaged $[\alpha]_D$ value of −172. Thus, TDDFT predicts that $[\alpha]_D$ is positive and negative for S,S-**1** and R,R-**1**, respectively.

The experimental $[\alpha]_D$ values of enantiomerically pure (+)-**1** and (−)-**1** in $CHCl_3$ solution were reported to be +72 and −71, respectively.[5] Adopting the AC S,S-(+)/R,R-(−) for **1**, the

(11) Matsuda-Sentou, W.; Shinmyozu, T. *Eur. J. Org. Chem.* **2000**, 3195.

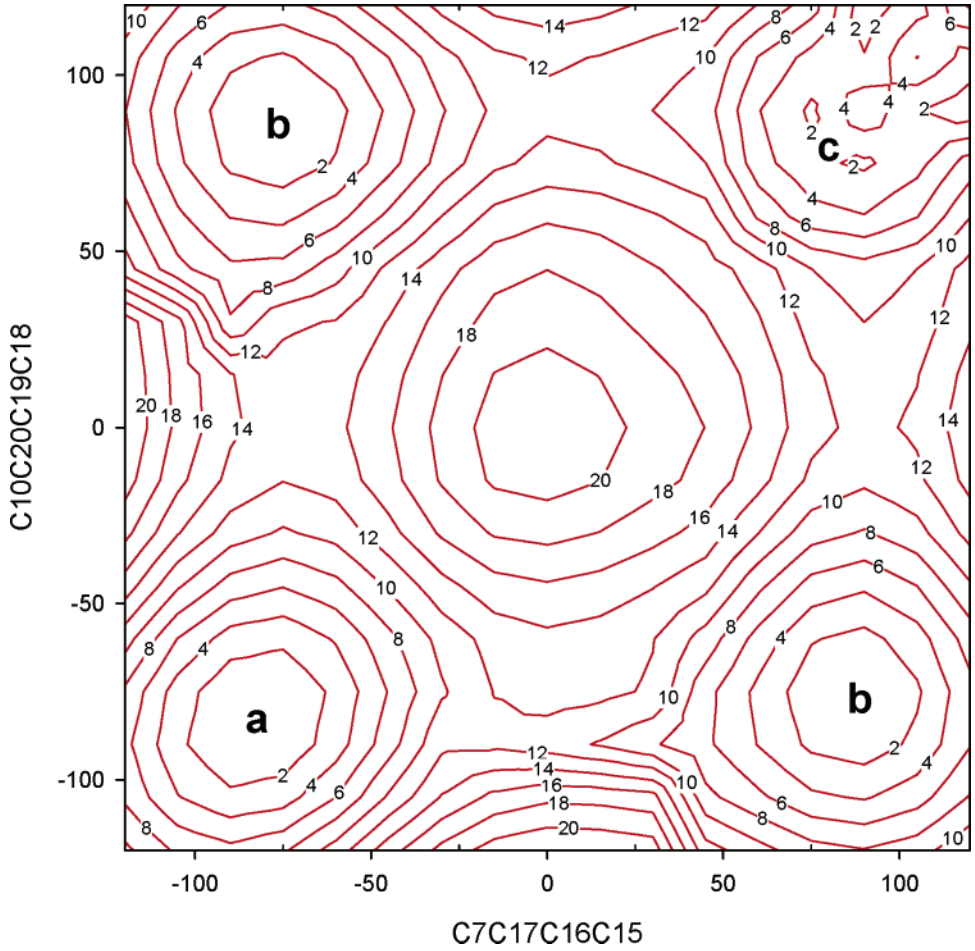

Figure 2. B3LYP/6-31G* potential energy surface of R,R-**1**. Contours are spaced by 2 kcal/mol.

Table 3. Comparison of Calculated and Experimental Dihedral Angles of **1**[a]

			C10–C20–C19–C18	C20–C19–C18–C4	C7–C17–C16–C15	C17–C16–C15–C1
(+)-**1**	**A**	exptl	89.3	−50.7	93.5	−52.3
		calcd (**c**)	88.4	−56.1	88.4	−56.1
	B	exptl	−84.0	63.3	−81.5	69.8
		calcd (**a**)	−82.6	63.4	−82.6	63.4
	C	exptl	90.2	−55.8	−72.8	76.6
		calcd (**b**)	87.2	−58.2	−76.7	70.2
	D	exptl (83A, 84A, 85A)[b]	−89.9	55.4	−81.6	63.3
		calcd (**a**)	−82.6	63.4	−82.6	63.4
	D	exptl (83B, 84B, 85B)[b]	92.3	−49.3	−81.6	63.3
		calcd (**b**)	87.2	−58.2	−76.7	70.2
(±)-**1**		exptl (18)[c]	82.3	−68.9	−87.3	63.2
		calcd (**b**)	87.2	−58.2	−76.7	70.2
		exptl (19)[c]	82.3	−68.9	52.0	−54.8
		calcd (**c**)	88.4	−56.1	88.4	−56.1

[a] In degrees. Experimental dihedral angles from structures of (+)-**1**[5] and (±)-**1**[11] (Cambridge Crystallographic Data Centre). Calculated dihedral angles are for B3LYP/6-31G* geometries. [b] Numbers in parentheses are numbers of disordered atoms in ref 5. [c] Number in parentheses is number of disordered atom in ref 11.

deviation between calculated and experimental $[\alpha]_D$ values is 100. If the AC were instead S,S-(−)/R,R-(+), the deviation would be 244. The S,S-(+)/R,R-(−) AC gives substantially superior agreement between calculated and experimental $[\alpha]_D$.

In order to examine the sensitivity of the calculated $[\alpha]_D$ values of the conformation of **1** to their equilibrium geometries, we have recalculated $[\alpha]_D$ using the structures for **a**, **b**, and **c** obtained from the X-ray analysis of (+)-**1**. The results obtained are given in Table 5. For conformations **a** and **b**, the magnitudes of $[\alpha]_D$ are significantly reduced; for **c**, the magnitude increases. In all cases the sign of $[\alpha]_D$ is unaffected. Recalculation of the conformationally averaged $[\alpha]_D$ using the same populations x_i as before leads to $[\alpha]_D = -109$ for R,R-1. The deviation from the experimental $[\alpha]_D$ is reduced to 37.

Circular Dichroism. We have predicted the electronic CD of **1** using the ab initio TDDFT methodology implemented in Gaussian 03. Excitation energies/wavelengths and rotational strengths of the four lowest excitations calculated using the B3LYP functional and the aug-cc-pVDZ basis set for each of the three conformations, **a**−**c**, are given in Table 6. For each conformation the B3LYP/6-31G* geometry is used. For all three conformations a low-energy excitation is predicted whose

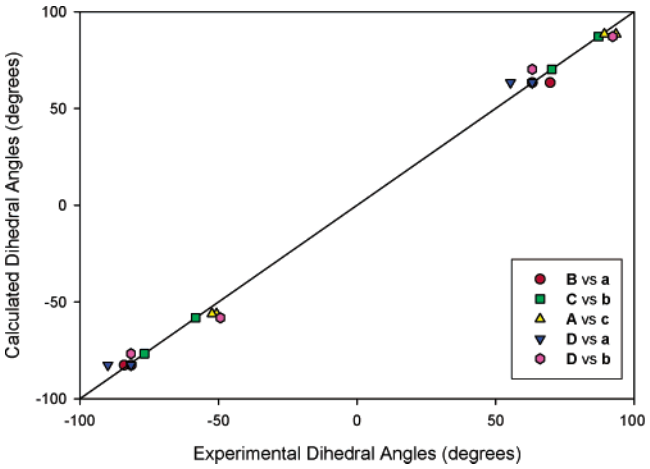

Figure 3. Comparison of calculated and experimental dihedral angles of R,R-**1** and (+)-**1**, respectively.

Table 4. Comparison of Calculated and Experimental Phenyl−Barrelene Distances[a]

	C7–C1	C12–C6	C11–C5	C10–C4	C9–C3	C13–C2
A						
exptl	3.260	4.051	3.381	3.302	4.008	3.310
calcd (**c**)	3.332	4.099	3.416	3.332	4.099	3.416
B						
exptl	3.295	4.066	3.353	3.233	3.904	3.280
calcd (**a**)	3.329	4.078	3.405	3.329	4.078	3.405
C						
exptl	3.195	3.919	3.312	3.277	4.000	3.285
calcd (**b**)	3.327	4.128	3.480	3.367	4.061	3.377

[a] In angstroms. Experimental distances from structure of (+)-**1**[5] (Cambridge Crystallographic Data Centre). Calculated distances are for B3LYP/6-31G* geometries.

Table 5. Specific Rotations, $[\alpha]_D$, of R,R-1 at B3LYP/6-31G* and X-ray Geometries[a]

	B3LYP/6-31G*				X-ray		
	a	**b**	**c**		**B**	**C**	**A**
$[\alpha]_D$	−235.4	−70.5	34.6	$[\alpha]_D$	−167.1	−21.3	95.4
	av[b]	−172			av[b]	−109	

[a] $[\alpha]_D$ values in deg [dm (g/cm^3)]$^{-1}$. [b] Average calculated using B3LYP/6-31G* ΔG-based populations (Table 1).

wavelength is >400 nm. The rotational strengths of this transition are negative for all three conformations of R,R-**1**. Higher excitations are predicted at λ < 350 nm.

The CD spectrum predicted for the equilibrium mixture of conformations, using B3LYP/6-31G* ΔG-based x_i values, is shown in Figure 4, together with the experimental spectra of (+)- and (−)-**1**.[5] We assign the broad, low-energy feature in the experimental CD spectrum, peaking at 354 nm (3.51 eV), to the lowest-energy excitations of **a**, **b**, and **c**. The predicted CD is negative for R,R-**1**, as is the experimental CD for (−)-**1**. The predicted, conformationally averaged rotational strength is -5.0×10^{-40} esu^2 cm^2; the experimental rotational strength is estimated to be $\sim -11 \times 10^{-40}$ esu^2 cm^2. This assignment therefore leads to the AC: S,S-(+)/R,R-(−), in agreement with the AC derived from $[\alpha]_D$. The assignment of the two bands at 270−280 nm in the experimental CD is less unambiguous. Assuming that they correspond to the second lowest excitations of conformations **a** and **b**, respectively, the positively signed CD of both bands for (−)-**1** is consistent with the predicted positive rotational strengths for R,R-**1**, leading to the same AC as obtained from the longer wavelength band.

Table 6. Electronic Excitation Energies and Rotational Strengths of R,R-1 at B3LYP/6-31G* and X-ray Geometries

	B3LYP/6-31G*					X-ray				
	ΔE (eV)	λ (nm)	R_{length}[a]	$R_{velocity}$[a]	f[b]	ΔE (eV)	λ (nm)	R_{length}[a]	$R_{velocity}$[a]	f[b]
a	2.93	423.0	−5.44	−5.12	0.0049	3.05	407.1	−5.45	−5.21	0.0046
	3.71	333.9	6.64	6.60	0.0018	3.88	319.9	6.96	6.90	0.0015
	3.86	321.1	−4.03	−3.92	0.0001	4.03	308.0	−5.05	−4.95	0.0007
	4.14	299.4	0.74	0.77	0.0012	4.29	289.0	0.25	0.29	0.0015
b	2.97	417.6	−5.22	−4.89	0.0050	3.10	400.0	−6.57	−6.24	0.0056
	3.74	331.2	4.81	4.77	0.0022	3.89	318.9	5.05	5.06	0.0031
	3.88	320.0	0.24	0.33	0.0000	4.05	305.8	4.56	4.59	0.0003
	4.16	298.1	−3.06	−3.03	0.0011	4.28	290.0	−1.66	−1.59	0.0010
c	2.95	420.0	−3.60	−3.27	0.0048	3.01	411.4	−1.06	−0.82	0.0042
	3.80	325.9	3.24	3.21	0.0015	3.95	313.7	2.08	2.05	0.0010
	3.98	311.6	−3.38	−3.14	0.0001	4.13	300.3	−5.09	−5.07	0.0004
	4.19	296.2	0.86	0.85	0.0011	4.40	281.9	1.16	1.17	0.0013

[a] Rotational strengths in 10^{-40} esu^2 cm^2. The excellent agreement of R_{length} and $R_{velocity}$ values demonstrates that basis set error is small for both values. [b] Oscillator strength.

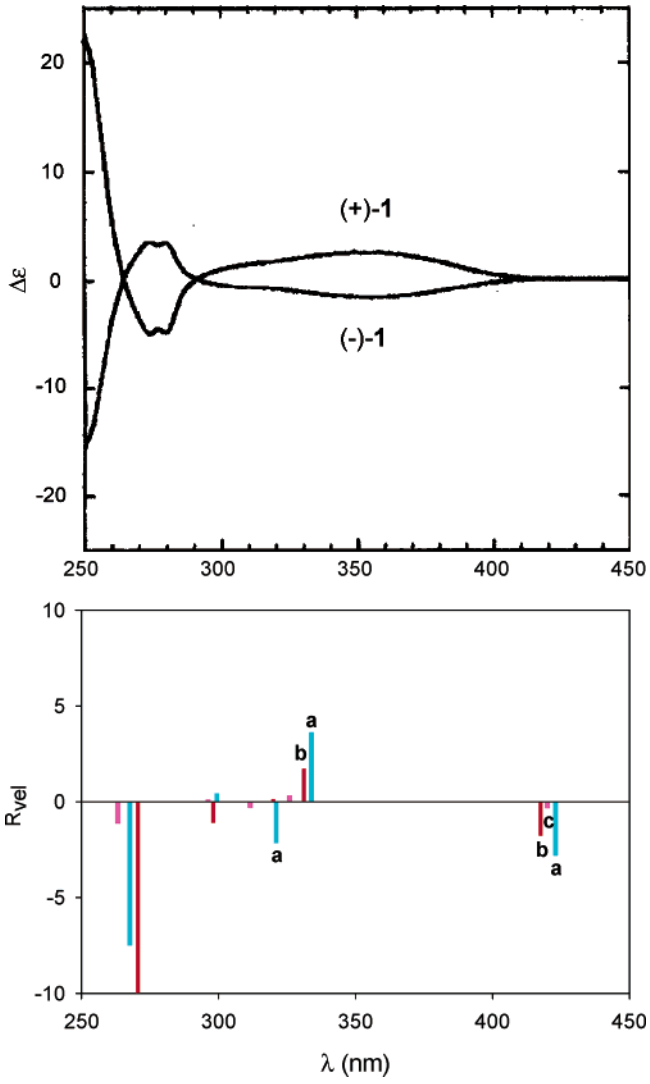

Figure 4. Calculated and experimental CD of **1**. Calculated rotational strengths are for R,R-**1**. Experimental spectra are from ref 5.

Matsuda-Sentou and Shinmyozu[5] identified the 354 nm transition of **1** as charge-transfer in nature. Specifically, on the

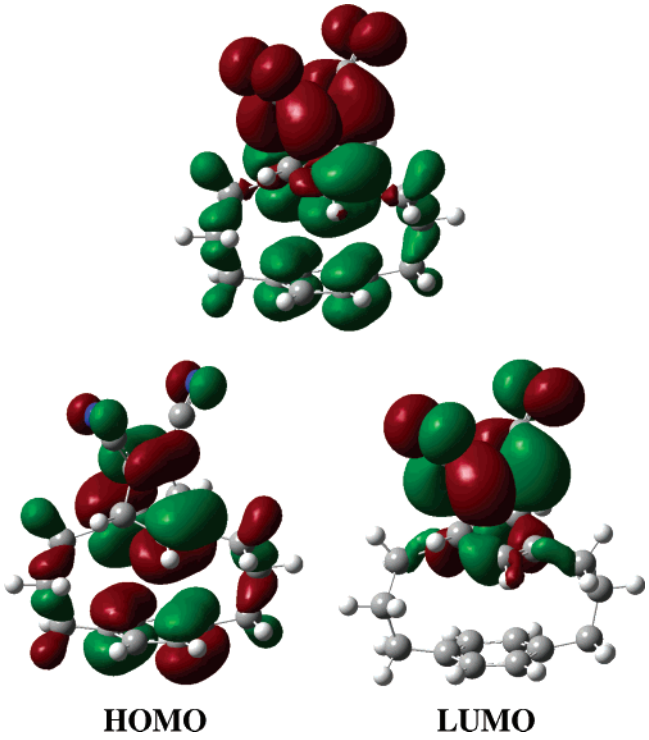

Figure 5. B3LYP/aug-cc-pVDZ//B3LYP/6-31G* HOMO and LUMO and the difference density between the ground and lowest excited state of conformer **a**. Red and green label positive and negative contributions to the HOMO and LUMO orbitals and the difference density.

basis of INDO/S calculations, the transition was assigned to an excitation from a π-HOMO of the benzene ring to a π*-LUMO of the dicyanoethylene moiety of the barrelene. This assignment is qualitatively supported by the TDDFT calculation. In all three conformations, the dominant contribution to the lowest electronic excitation is from the HOMO → LUMO excitation. The HOMO and LUMO orbitals of conformation **a** are displayed in Figure 5, together with the ground to excited state difference density.[12] The latter clearly shows that in the lowest excitation charge flows from the phenyl moiety to the dicyanoethylene moiety of the barrelene group.

As with the $[\alpha]_D$ calculations, we have examined the sensitivity of the calculations of the electronic excitation energies and rotational strengths to the choice of geometry by substituting the X-ray structures of conformations **a**, **b**, and **c** for the B3LYP/6-31G* structures, with the results given in Table 6. For all three conformations, the energies of the lowest excitations are increased by ~0.1 eV, in better agreement with experiment. The changes in rotational strengths are small.

Discussion

The barrelenophane, **1**, is a flexible molecule. The two three-carbon bridges connecting the barrelene and phenyl moieties are nonplanar and can each adopt more than one conformation. Conformational analysis—i.e., the definition of the structures and relative energies of the stable conformations—of **1** is a prerequisite for analysis of the chiroptical properties of **1**. In this work, we have adopted two approaches to defining the stable conformations of **1**. Firstly, we have carried out Monte Carlo conformational searching using both a molecular mechanics method (MMFF94) and a semiempirical method (AM1). At the present time, Monte Carlo searching using ab initio methods is impractical. MMFF94 and AM1 yield the same qualitative conclusion: there are three stable conformations of **1**, two of C_2 symmetry, and one of C_1 symmetry. These structures have been further optimized using DFT at the B3LYP/6-31G* level. B3LYP/6-31G* frequency calculations confirm that all three conformations are indeed stable (i.e., PES minima). Secondly, we have carried out a 2D scan of the B3LYP/6-31G* PES, varying simultaneously the two dihedral angles C7C17C16C15 and C10C20C19C18. The PES obtained (Figure 2) exhibits four valleys. The two C_2 structures previously obtained lie within two of these valleys. The remaining two valleys correspond to two identical C_1 structures which are interconverted by a 180° rotation. Thus, the 2D scan yields an identical outcome to the Monte Carlo searching.

The MMFF94, AM1, and B3LYP/6-31G* methods yield different structures and relative energies for the three conformations of **1**: **a**, **b**, and **c**. The B3LYP/6-31G* method is the most reliable and predicts the energy ordering **a** < **b** < **c**. MMFF94 predicts the same ordering; however, the spread of energy is considerably less than predicted by B3LYP/6-31G*. AM1 predicts a qualitatively different ordering; **c** < **a** ≈ **b**. This finding is not unexpected and further confirms the lesser reliability of the AM1 method in predicting conformational energetics.[13] Based on the B3LYP/6-31G* relative energies, Boltzmann statistics predicts a population distribution of **a**:**b**:**c** = 55:36:10% at room temperature. The use of free energies is more correct in predicting populations, and we have therefore calculated relative free energies at the B3LYP/6-31G* levels. Relative ΔG values exhibit a larger spread than do the relative ΔE values, with the result that the population distribution predicted thence exhibits a higher percentage for conformer **a**: **a**:**b**:**c** = 65:30:6%.

The accuracy of theoretical predictions of the conformational structures of a flexible molecule can be gauged by comparison to experimental structural data, when available. In the case of **1**, X-ray crystallography has been carried out for both (+)-**1** and racemic-**1**. In general, conformationally flexible molecules crystallize in a single conformation, most commonly the lowest energy conformation in solution. It is then only possible to make comparison of theory and experiment for one conformation. However, in the case of (+)-**1**, it turns out that all three stable conformations are present in the crystal structure. There are four inequivalent molecules in the unit cell, labeled **A**, **B**, **C**, and **D** by Matsuda-Sentou and Shinmyozu, who reported that the "four molecules of **1** have almost the same structures, but one carbon bridge chain of the molecule **D** is disordered". Closer examination shows that each of the three molecules **A**, **B**, and **C** in fact exhibit one of the three predicted conformational structures of **1**, while the disordered molecule **D** is a superposition of two conformations. Specifically, molecules **A**, **B**, and **C** can be identified with conformations **c**, **a**, and **b**, respectively, while molecule **D** is a superposition of conformations **a** and **b**. Thus, remarkably, in crystalline (+)-**1** all three stable conformations

(12) The difference density is the difference between the ground-state density and the unrelaxed excited-state density formed from the CI one-particle density matrix (Foresman, J. B.; Head-Gordon, M.; Pople, J. A.; Frisch, M. J. *J. Phys. Chem.* **1992**, *96*, 135). Note that the unrelaxed excited state density constructed in this way only recovers some of the gross features of charge redistribution in the excited state, as orbital relaxation effects are not included.

(13) Hehre, W. J. *A Guide to Molecular Mechanics and Quantum Chemical Calculations*; Wavefunction Inc., Irvine, CA, 2003; Chapter 8.

of **1** are present. Quantitative comparison of structural parameters predicted for **a**, **b**, and **c** to the X-ray values for **B**, **C**, and **A** shows the expected level of agreement for the B3LYP/6-31G* method (Table 3 and Supporting Information). The experimental X-ray structures thus provide strong support for the correctness of the DFT conformational analysis.

At the present time, there are no data providing experimental values for the relative energies of the conformations of **1**. In this work, we have used the B3LYP/6-31G* free energy differences to obtain the percentage populations of the conformations of **1** in room-temperature solution. We recognize the limitations of these values originating from errors in the functional, incompleteness of the basis set and the absence of the solvent in our calculations. Experimental measurements—for example, variable-temperature NMR measurements[14]—of relative free energy differences would be of assistance in evaluating the accuracy of our predicted values.

The specific rotations of conformers **a**, **b**, and **c** have been calculated using TDDFT. The combination of the B3LYP functional and aug-cc-pVDZ basis set has been shown to provide $[\alpha]_D$ values for a wide range of rigid organic molecules in excellent agreement with experimental values: over 30 molecules, the average absolute error was 23.1.[1a] We have therefore used this functional and basis set in predicting $[\alpha]_D$ for **1**. The use of GIAOs in the TDDFT methodology implemented in Gaussian 03 guarantees origin-independent specific rotations, an essential requirement for meaningful comparison to experiment. As in flexible molecules previously studied,[3a,b] the specific rotation is a sensitive function of conformation. For **a** and **b**, $[\alpha]_D$ is of the same sign but of very different magnitude. For **c**, the sign and magnitude are different. The conformationally averaged $[\alpha]_D$ value is dominated by the contributions of conformers **a** and **b**, since they account for >90% of the population at room temperature. As a result, the predicted sign of $[\alpha]_D$ is negative for the R,R AC, irrespective of the relative populations of **a** and **b**. Using B3LYP/6-31G* ΔG-based populations, $[\alpha]_D$ is predicted to be −172. We therefore predict the AC of **1** to be S,S-(+)/R,R-(−). On this basis, the difference between the calculated and experimental $[\alpha]_D$ values is 100.

The difference between predicted and observed $[\alpha]_D$ values is considerably greater than the average difference found in our earlier benchmark study.[1a] There are several possible reasons for this. Firstly, the predicted $[\alpha]_D$ may be particularly sensitive to the geometry used, and the use of the B3LYP/6-31G* geometry may cause significant error in $[\alpha]_D$. While we have shown that the B3LYP/6-31G* geometries of **a**, **b**, and **c** are in good overall agreement with the experimental geometries, they are not identical. In particular, as discussed above, significant differences (∼0.1 Å) are found in the distances defining the separation of the barrelene and phenyl moieties. These may or may not originate in crystal packing effects and exist in solution. However, in order to gauge the sensitivity of calculated $[\alpha]_D$ values to geometry, we have recalculated $[\alpha]_D$ for **a**, **b**, and **c** using the X-ray coordinates. A substantial reduction in the magnitudes of the $[\alpha]_D$ values of **a** and **b** occurs, together with an increase in the magnitude for **c**. Using the same ΔG-based populations as before, the conformationally averaged $[\alpha]_D$ value decreases to −109 and the difference from experiment decreases to 37. We conclude that at least some fraction of the error in the $[\alpha]_D$ values obtained using B3LYP/6-31G* geometries could well be attributable to errors in the geometries. Secondly, the difference in calculated and experimental $[\alpha]_D$ values may originate in errors in the populations of **a**, **b**, and **c** used for conformational averaging. We have discussed this issue in detail in a previous publication.[3b] In the case of **1**, a decrease in the population of **a**, with corresponding increases in the populations of **b** and **c**, will lead to a less negative $[\alpha]_D$. Thus, if the relative free energies of **b** and **c** are decreased, $[\alpha]_D$ will be in better agreement with experiment. Thirdly, the predicted $[\alpha]_D$ may be particularly sensitive to the density functional used. We have found that in some molecules, large changes in $[\alpha]_D$ occur when the B3LYP functional is replaced by the less accurate BLYP functional[15] (although for many molecules very similar results are obtained). It turns out that such sensitivity exists for **1**: $[\alpha]_D$ for conformation **a** of R,R-**1** is −522 when BLYP is used, in contrast to the B3LYP value of −235. Thus, it is very possible that further improvement of the functional beyond B3LYP will lead to further reduction in $[\alpha]_D$ and, consequently, to better agreement with experiment. Further light on this issue is shed by the comparison of the predicted and experimental CD, to which we now turn.

The excitation energies and rotational strengths of the lowest excited electronic states of the conformers **a**, **b**, and **c** of **1** have been calculated using TDDFT. The combination of the B3LYP functional and the aug-cc-pVDZ basis set has been used for consistency with the calculations of $[\alpha]_D$. For all three conformers, we predict that the lowest excited electronic state has an excitation energy of 2.9−3.0 eV, corresponding to wavelengths ∼420 nm. The predicted rotational strengths are negative in all cases for R,R-**1** and similar in magnitude. Thus, whatever the percentage populations of the individual conformations, we predict low-energy, negative CD for R,R-**1**. The experimental CD spectrum exhibits a broad near-UV band at 354 nm (3.51 eV); the CD is negative for (−)-**1**. Qualitatively, theory and experiment are in agreement if the AC is S,S-(+)/R,R-(−). Thus, the CD spectrum of **1** leads to the same AC as obtained from $[\alpha]_D$.

The ∼360 nm absorption and CD of **1** are noticeably broad. In part, this can be attributed to the contributions of more than one conformer, with somewhat different excitation energies. More important, however, is the nature of the transition. On the basis of INDO/S calculations, Matsuda-Sentou and Shinmyozu assigned this band as a charge-transfer transition, involving the HOMO of the phenyl moiety and the LUMO of the dicyano barrelene moiety, and our TDDFT calculations support this assignment. Charge-transfer transitions are commonly broad. That the ∼360 nm absorption and CD of **1** are broad is consistent with their assignment to a charge-transfer transition.

Our TDDFT calculations predict excitation energies for the conformers of **1** smaller than the observed excitation energy by ∼0.5 eV. This is not unprecedented.[16] In addition, TDDFT

(14) Sakamoto, Y.; Miyoshi, N.; Hirakida, M.; Kusumoto, S.; Kawase, H.; Rudzinski, J. M.; Shinmyozu, T. *J. Am. Chem. Soc.* **1996**, *118*, 12267.

(15) For example, B3LYP $[\alpha]_D$ values (calculated using the aug-cc-pVDZ basis set and at B3LYP/6-31G* geometries) are −1216 for norbornenone and −342 for Tröger's Base.[1a] Using BLYP in place of B3LYP yields −1762 and −615, respectively (unpublished results).

(16) See, for example, ref 1g wherein absorption and CD spectra calculated using TDDFT for several helicenes are blue-shifted by 0.45 eV to optimize agreement with experimental spectra.

Table 7. Comparison of Lowest Excitation Contributions to $[\alpha]_D$ Using Calculated and Experimental Excitation Energies

	λ (nm)			$[\alpha]_D$[d]	
	calcd[a]	exptl[b]	$R_{velocity}$[c]	calcd λ	exptl λ
a	423.0	354	−5.12	−159	−85
b	417.6	354	−4.89	−144	−81
c	420.0	354	−3.27	−99	−54

[a] B3LYP/aug-cc-pVDZ//B3LYP/6-31G* values from Table 6. [b] Reference 5. [c] B3LYP/aug-cc-pVDZ//B3LYP/6-31G* values from Table 6. Rotational strengths in 10^{-40} esu^2 cm^2. [d] Contribution to $[\alpha]_D$ of the lowest excitation, calculated using calculated and experimental λ values.

may not perform well for charge-transfer transitions.[17] Improved agreement between calculated and experimental excitation energies requires functionals superior in accuracy to B3LYP.

The accuracy of the calculated excitation energies is relevant to the accuracy of the calculated specific rotation, $[\alpha]_D$. As is well-known,[18] the transparent spectral region specific rotation can be written as a sum over all electronic excitations, in the form:

$$[\alpha]_\lambda = \left(\frac{9147}{M}\right)\sum_i\left(\frac{R_i\lambda_i^2}{(\lambda^2-\lambda_i^2)}\right)$$

where R_i is the rotational strength of the *i*th excitation in 10^{-40} esu^2 cm^2. Errors in calculated excitation wavelengths, λ_i, thus cause errors in calculated $[\alpha]_\lambda$ values. For the *i*th excitation the error in $[\alpha]_\lambda$ is greater, the smaller is $\lambda^2 - \lambda_i^2$, i.e., the closer λ_i is to the experimental wavelength λ. We have examined the errors in the predicted $[\alpha]_D$ values of the conformers of **1** resulting from the errors in predicted excitation energies for the lowest, charge-transfer excitations, with the results given in Table 7. For conformations **a**, **b**, and **c** the contributions to $[\alpha]_D$ from the lowest excitation, obtained from the calculated excitation energies and rotational strengths, are −159, −144, and −99, respectively. Recalculation using the experimental wavelength reduces these values to −85, −81, and −54. Thus, the errors in the calculated $[\alpha]_D$ values originating in errors in the excitation energies of the lowest excitation alone are 74, 63, and 45, respectively. Recalculation of the conformationally averaged $[\alpha]_D$ value using $[\alpha]_D$ values for **a**, **b**, and **c** reduced by these amounts leads to a "corrected $[\alpha]_D$" of −102, a value considerably closer to the experimental value. We conclude that the errors in the calculated excitation energies of the lowest transition can cause significant error in the calculated $[\alpha]_D$. These excitation energies are very sensitive to the functional used. With BLYP, the excitation energy is 2.34 eV (529 nm) for **a**. Thus, as the functional is improved from BLYP to B3LYP the excitation energies are substantially more accurately predicted. Further improvement in the functional should lead to even better agreement and, consequently, enhance the accuracy of the predicted $[\alpha]_D$.

The ACs arrived at from the specific rotation $[\alpha]_D$ of **1** and from the near-UV circular dichroism of **1** are the same: S,S-(+)/R,R-(−). The consistency of the outcomes from the two chiroptical phenomena strongly supports the reliability of the AC. That is, the reliability of the AC is substantially greater than would be the case if only one of the two phenomena were used. We believe that future applications of TDDFT to the determination of AC will be greatly enhanced if both optical rotation and circular dichroism are considered together.

This work also serves to illustrate the considerable advantages of chiroptical methods for determining AC relative to the Bijvoet X-ray method. The determination of AC using X-ray crystallography requires diffraction-quality crystals and, traditionally, a "heavy atom". While ACs can sometimes be determined for molecules lacking "heavy atoms", this is not always possible and, in some cases, yields an incorrect result.[19] In the case of **1**, which lacks "heavy atoms", crystals of (+)-**1** were obtained, but the AC could not be reliably determined. In contrast, measurement of optical rotation and circular dichroism is carried out in solution, so that crystals are not prerequisite. The measurements are routine with commercial instrumentation. The TDDFT calculations are now also routine using widely distributed commercial software. Both experimental and theoretical methods are general and do not require "heavy atoms". Thus, considerably less effort is required for the determination of AC using optical rotation and circular dichroism, and the methodology is more generally applicable.

Historically, the majority of ACs have been determined by synthesis from precursors of known AC using reactions of well-defined stereochemistry. In such cases, direct determination of the AC of the molecule of interest is unnecessary. However, enantiomers of chiral molecules are increasingly prepared by resolution of racemic mixtures, especially via chiral chromatography. In such cases, ACs are not defined via the method of preparation, and subsequent determination is necessary. The barrelenophane **1** is an example of a chiral molecule first resolved using chiral chromatography. In this and analogous situations, chiroptical methods for determining AC are of especial value.

Conclusion

We have illustrated the concerted application of TDDFT calculations of transparent spectral region electronic optical rotation and electronic circular dichroism to the determination of AC via the chiral barrelenophane **1**, the first optically active barrelenophane to be prepared. The methodology is quite general and should find wide application to chiral organic molecules.

Acknowledgment. We are grateful to NSF for a grant to P.J.S. (Grant CHE-0209957) and to the USC Center for High Performance Computing for computer time.

Supporting Information Available: Comparison of calculated and experimental bond lengths and bond angles for conformers **a**−**c** of molecule **1**. Text files containing B3LYP/6-31G* optimized geometries in Cartesian coordinates of molecule **1**. This material is available free of charge via the Internet at http://pubs.acs.org.

JA049185Q

(17) Tozer, D. J.; Amos, R. D.; Handy, N. C.; Roos, B. O.; Serrano-Andres, L. *Mol. Phys.* **1999**, *97*, 859.
(18) Djerassi, C. *Optical Rotatory Dispersion*; McGraw-Hill: New York, 1960; Chapter 12 by A. Moscowitz, p 166.
(19) See, for example, the case of 2-(1-hydroxyethyl)-chromen-4-one; ref 3b.